

THERMAL-HYDRAULIC ANALYSIS OF A 7-PIN SODIUM FAST REACTOR FUEL BUNDLE WITH A NEW PATTERN OF HELICAL WIRE WRAP SPACER

Seong Dae Park, Sung Bo Moon, Seok Bin Seo, In Cheol Bang*

School of Mechanical and Nuclear Engineering,
Ulsan National Institute of Science and Technology (UNIST)
50 UNIST-gil, Ulsan-gun, Ulsan, 689-798, Republic of Korea
sdpark@unist.ac.kr, sbmoon@unist.ac.kr, sbseo@unist.ac.kr, icbang@unist.ac.kr

ABSTRACT

Thermal-hydraulic analysis was conducted of a 7-pin fuel bundle by using CFD. Currently, wire-wrapped spacers are wound on the fuel pins in the same direction. Counter flow is predicted to occur in all sub-channels due to this pattern. This flow was confirmed in this work as well as previous research. Complicated flow formed locally around the wire-wrapped pins. A new type of arrangement for wire-wrapped spacers, called the U-pattern, is presented to provide favorable flow for coolant mixing. In this pattern, 7 pins are designated as one group, the center pin has no wrapping, and the pins surrounding the center pin have alternate winding directions. Superior mixing effect and ideal flow pattern were confirmed in CFD analysis. The maximum temperature in the 7-pin fuel bundle was about 30° cooler than that of the ordinary wire-wrapped fuel bundle. Pressure drop for the U-pattern was reduced by approximately 10% compared with the ordinary pattern. CFD results show that U-pattern could satisfy the requirements for heat transfer enhancement and reduced pressure drop simultaneously.

KEYWORDS

Sodium-cooled fast reactor, wire wrapped spacer, CFD, sub-channel

1. INTRODUCTION

A liquid-metal fast breeder reactor (LMFBR) has an attractive neutron utilization factor, in comparison with thermal reactors. Fast reactors could provide sustainable nuclear power and effective actinide management by using the fissionable uranium resource and fast neutrons. One of the noticeable differences between the fast reactor and the thermal reactor is the length of the mean free path. A fast reactor has a relatively long mean free path, or low macro absorption cross-section, due to the use of fast neutrons. Loading of high enrichment fuel is required to maintain continuous fission in a fast reactor. The neutron characteristics of a fast reactor means that the core geometry is small, and therefore the sub-channels between the fuel pins are narrow. Therefore, many researchers have studied how to effectively remove generated heat, within the geometrical limitations.

Wire-wrapped pins have been presented as a solution to provide a clear sub-channel for coolant flow and enhance the heat transfer between the fuel pins and coolant. Related research has been performed in order to understand the effects of wire-wrapping a pin. The general idea is that a helical wire wrapping forces the fluid to rotate around fuel pins. A swirling flow could be formed, causing the temperature gradient of the coolant to be uniform. However, a helical wire wrapping could increase the pressure drop that is required to maintain constant flow in a sub-channel. Many researchers have attempted to understand and model the characteristics and pressure drop of wire-wrapped spacers.

Novendstern developed a semi-empirical model to predict pressure drop in a wire-wrapped fuel pin bundle [1]. This model is able to predict the value of pressure drop within 14% over a wide range of geometries in the turbulent flow regime.

Cheng and Todreas developed hydrodynamic models of wire-wrapped rod bundles to calculate sub-channel friction factors and mixing parameters for use in sub-channel analysis codes [2]. Both flow regime and geometry effects were taken into account in these models. Correlations based on the models for the sub-channel friction factor and mixing parameters were calibrated with the available data at that time. These correlations provide some background information suitable for validation.

Gajapathy et al. investigated the sodium flow and temperature distributions in heat-generating fuel pin bundles with helical spacer wires [3]. The characteristics of 7, 19, and 37 fuel pin bundles were analyzed by using a commercial computational fluid dynamics (CFD) code. It was found that the normalized outlet velocities were nearly equal to unity, even in the peripheral and central zones (in the range 0.9–1.1), and there was good agreement with published hydraulic experimental measurements.

Hamman and Berry evaluated a CFD model and simulation for large-scale problems of a fast reactor with wire-wrapped pin bundles [4]. Three-dimensional flow distributions of sodium in the sub-channels of a 19-pin fuel bundle were simulated by using a commercial CFD code. Their results have a difference of 9–15% in comparison with some correlations.

Volkov et al. developed a CFD model of a 19-rod wire-wrapped pin fuel bundle [5]. They found that the use of the high-Reynolds $k-\varepsilon$ turbulence model for simulating the flow in the pin fuel bundle made it possible to reduce the dimension of the computational mesh, and hence perform a full-scale simulation of a fuel bundle. The obtained results are in good agreement with the empirical dependences and international calculations.

Talebi et al. conducted a parametric study of the Rayleigh number, inlet temperature and heat fluxes on the fluid flow and heat transfer inside the sub-channel with a CFD code that solves the governing equations with a finite volume method and SIMPLE algorithm [6]. The wire wrapped spacers created a uniform fluid velocity and temperature in the cross-section of the channel.

Currently, wire-wrapped spacers are wound in the same rotating direction. It might be estimated that the direction of swirl flow around the pins would be same. However, the direction of a cross flow in the center of a sub-channel on a perpendicular cross-section is uncertain, due to counter flow. A flow pattern of this sort would be unsuitable for creating a uniform temperature distribution in a coolant channel. In this work, a new helical wire-wrapped arrangement was studied, as part of an effort to improve the performance of wire wrapping based on the thermal hydraulics.

2. WIRE WRAP MODELS

2.1. Characteristics of ordinary wire-wrapped pin

Figure 1 shows the ordinary geometry of wire-wrapped fuel pin in an LMFBR. A number of fuel pins are located in the hexagonal walls. This wire wrap supports the separated geometry and makes a specific coolant channel between the pins. Figure 2 shows a possible flow of the coolant. The swirl flow enhances mixing of the coolant, which causes a uniform coolant temperature. Therefore, the temperature of the heated surface is decreased due to an enhanced heat transfer rate. Ultimately, the wire wrapping lowers the maximum temperature of a pin.

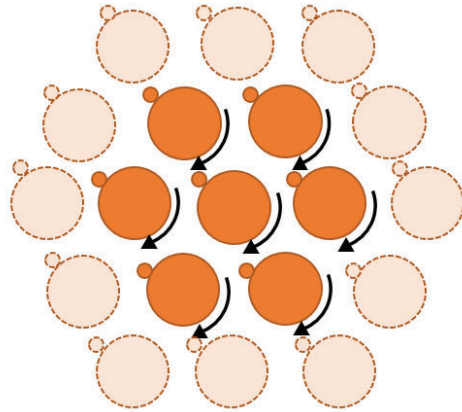


Figure 1. Geometry of ordinary wire-wrapped pins and flow pattern in sub-channels.

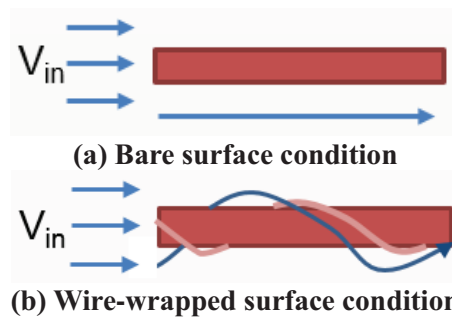


Figure 2. Estimated different flows around a pin

2.2. New wire-wrap arrangement and characteristics

Wire is wrapped on an ordinary fuel pin in an LMFBR with the same winding direction. The reason for this geometry may be due to the convenient manufacture and installation of wire wrap. However, a hydrodynamic issue can be detected in this arrangement. The flow direction rotating around the pins could be predicted as shown in figure 1. After examining figure 3, some concerns might arise about the flow pattern. The flow direction between the pins would be determined by the neighboring wire wrap. Because the position of the wire wrap continuously changes along the axial direction, a unique flow pattern would be formed in the fuel bundle, corresponding to the elevation of the fuel pin. However, it is not important to estimate the flow direction. The most critical point is that counter flow is formed in all sub-channels in the fuel bundle, and the coolant flow would be disturbed by counter flow of this sort. This phenomenon could result in negative effects on the heat transfer and pressure drop.

A new wire-wrapped pin arrangement was presented to solve the problem related to counter flow. 7 pins are designated as one group without the hexagonal walls. The center pin has no wire wrap, and the pins surrounding the center pin have sequentially different winding directions. We call this new wire-wrapped arrangement the U(UNIST)-pattern. Although there is no wire wrap around the center pin, all pins are definitely separated from each other. The axial movement of the pin is limited because both ends of the pin is fixed regardless of the wire wrapped spacer. The wire wrapped spacer is attached to prevent the contact between the pins. The length of the pin is long enough. The vibration of the pin is generated due to the coolant flow. The wire wrapped spacer suppressed this vibration. If there is not a wire wrapped spacer in the central pin in the 7-pin group, additional devices are not required to fix the pin axially. Figure 4 shows this pin arrangement the resulting flow characteristics. An ideal flow pattern could be

formed in presented pin arrangement. An enhanced mixing effect and decreased pressure drop are predicted because of the stable flow pattern. The maximum temperature of fuel pin could be reduced due to the well-mixed coolant. The decreased pressure drop makes it possible to increase the coolant flow condition with the same performance from the pumps. The range of plant operation condition could be extended to obtain improved efficiency and safety in an LMFBR.

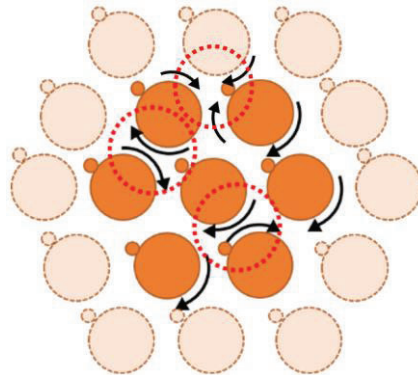
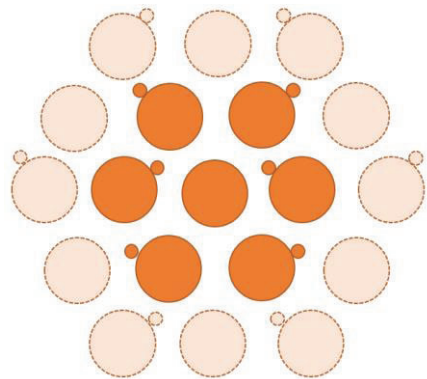
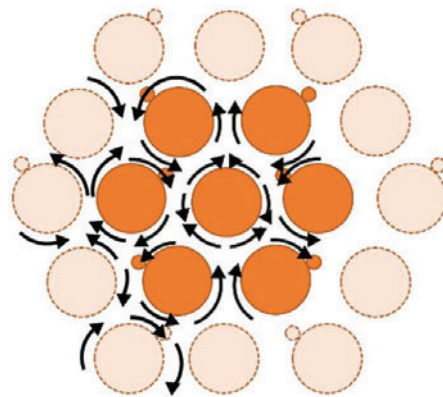


Figure 3. Postulated counter flow between the pins in sub-channels.



(a) New pin arrangement



(b) Estimated flow pattern

Figure 4. New pin arrangement (U-pattern).

3. CFD ANALYSIS

3.1. Geometry and boundary condition

CFD (ANSYS-CFX) simulation was conducted to analyze the presented pin arrangement. The dimensions of the pin and pitch were determined from the reference regarding KALIMER-600 as shown in Table I [7, 8]. KALIMER-600 is a fast neutron spectrum reactor that uses liquid sodium as a coolant. It has a capacity of 600MWe. The core generates fission heat of 1523.4MWt and is loaded with metal fuels of U-TRU-Zr. KALIMER - 600 is a pool-type reactor and all the primary sodium is contained in a reactor vessel. A 7-pin fuel bundle is the basic geometry. Thin 3 meshing layers was formed on the wall to reflect the effects of the friction. We used the tetrahedral mesh to describe the asymmetric geometry of subchannels. Mesh quality is more than 0.6. The option of volumetric heat generation was selected in order to simulate heat production caused by fission. The generated heat ratio varies according to the elevation of the fuel pin, as shown in figure 5. This value was calculated from the neutron flux profile in the axial direction. The geometry consists of metallic fuel (U-Pu-Zr), HT-9 cladding, and sodium coolant. Constant thermal and physical properties were determined for each material by considering the operation condition. The inlet velocity and temperature of sodium flow is 3.6 m/s and 390 °C, respectively. A k- ϵ turbulent model was selected to predict the behavior of sodium coolant. It is described that this turbulent model is an appropriate model to simulate the sub-channels with the wire wrapped pins in the study of Volkov et al. Model sensitivity study was required in this work. However, this work is focused to confirm some effects of wire spacer arrangement. The side surface of fuel bundle is a smooth wall with no slip and adiabatic boundary conditions. There are three types of geometry, as shown in figure 6. The effects of wire-wrapped pin arrangement could be distinguished through analysis of the three types of geometry

Table I. Geometry of bundle.

	Dimension (mm)
Fuel slug length	940
Fuel pin diameter	6.96
Cladding thickness	1.02
Pin pitch	10.5
Wire wrap diameter	1.4
Wire wrap pitch	204.9

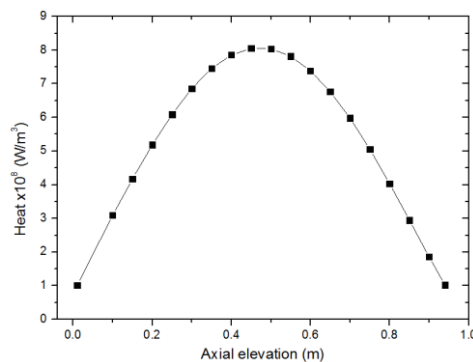
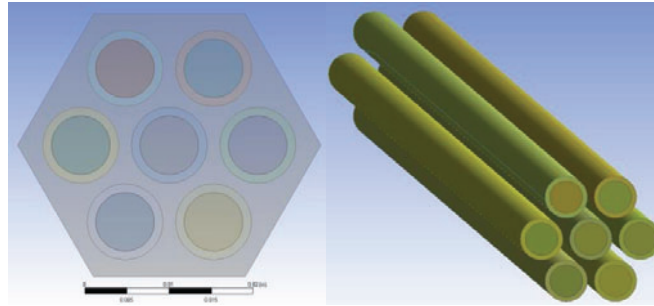
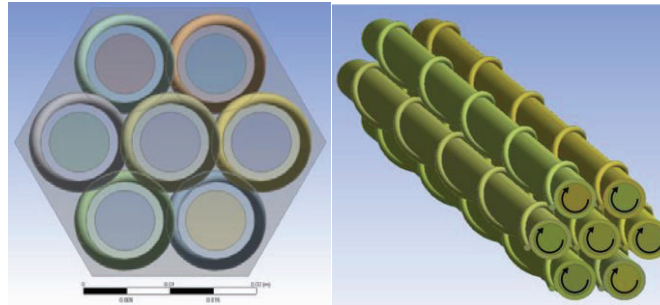


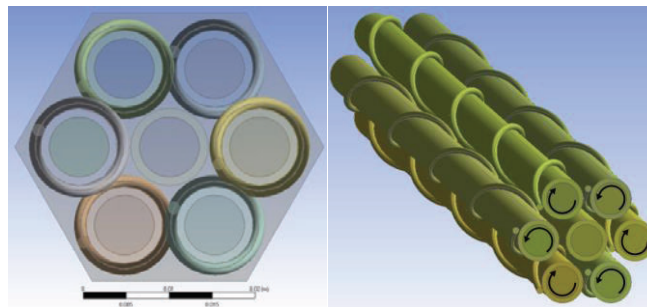
Figure 5. Axial power distribution at peak assembly.



(a) Non-wrapped



(b) Ordinary wire wrap



(c) U-pattern wire wrap

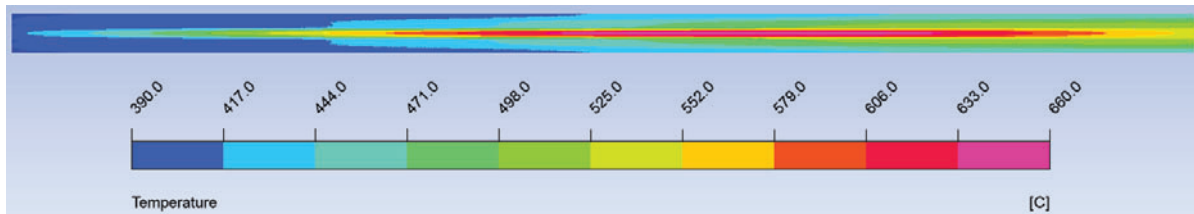
Figure. 6. The geometry of a 7-pin fuel bundle.

3.2. Temperature distribution in the bundle

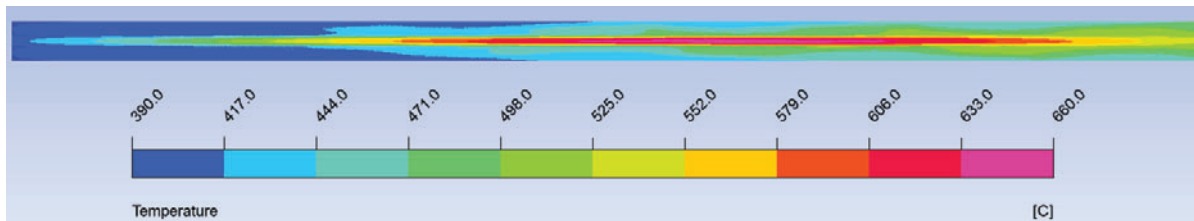
Figure 7 shows the temperature distribution on a perpendicular cross section for all the geometries. The trend of temperature distribution was determined by neutron flux, coolant velocity, and material of fuel. The metallic fuel was designed to load as the fuel material in KALIMER-600. Metallic fuel has high thermal conductivity in comparison with the oxide fuel. It is well known that the position of maximum temperature in a metallic fuel pin is higher than in an oxide fuel, because of considerable heat transfer in the axial direction through the pin. In all the CFD results, the position of maximum temperature for fuel pin is higher than the middle elevation of pin, as shown in figure 8 with one legend which has the same data range. It is suitable to understand the location and approximate maximum temperature value in three cases. The value of maximum temperature is different for the same elevation. The temperature distribution at a height of 0.8 m could provide important information to understand this characteristic. A relatively high position was selected as the reference height to confirm the mixing effect of the sodium coolant. When the ordinary wire is wrapped around the fuel pin, the temperature reduction is

approximately 8 °C. The trend of temperature distribution shown in figure 8(b) is similar to the trend in a previous study [3]. A surprising result is indicated in figure 7(c); a huge temperature reduction was observed. The hottest sodium coolant is concentrated in the center of fuel bundle for both the non-wrapped and the ordinary wire wrap cases. However, the maximum temperature regions were observed at some channels away from the center in the case of the U-pattern pin arrangement. The flow direction in these channels is out from center pin. The difference between maximum and minimum temperature is the smallest in this case. This means that mixing effect of the U-pattern is superior to that of the other cases. The coolant flow direction could be estimated from analysis of the interesting temperature pattern indicated in figure 7(c). The sub-channel around the center has the most dangerous condition, considering the heating boundary. The present pin arrangement is favorable for mixing and dissipating the heated sodium coolant around the center pin.

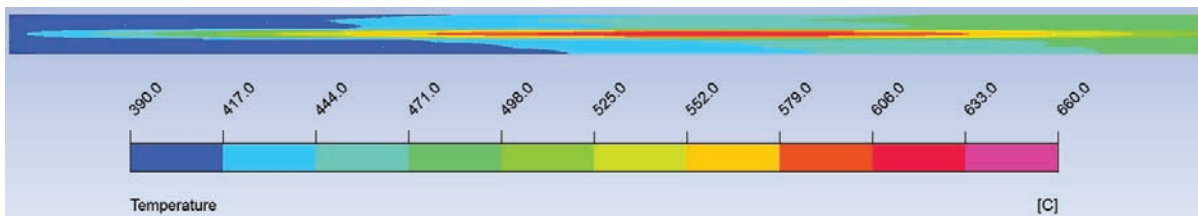
CFD simulation was conducted with only a 7-pin fuel bundle geometry. Therefore, the obtained results and insight could be limited for understanding the performance of wire wrap because of the relative small geometry that was used. However, this heat transfer trend could be extended to a larger size of fuel bundle, as shown in figure 4. Superior mixing effect and ideal flow pattern will be estimated in all sub-channels regardless of the fuel bundle size. Therefore, it is clear that the maximum temperature of core could be reduced when the U-pattern is utilized in the fuel bundle. By use of this arrangement, it is possible to ensure the safety of an LMFBR by decreasing the maximum temperature, or enhance the efficiency by increasing the operation coolant temperature.



(a) Non-wrapped



(b) Ordinary wire wrap



(c) U-pattern wire wrap

Figure 7. Temperature distribution of perpendicular cross section at different sub-channel conditions.

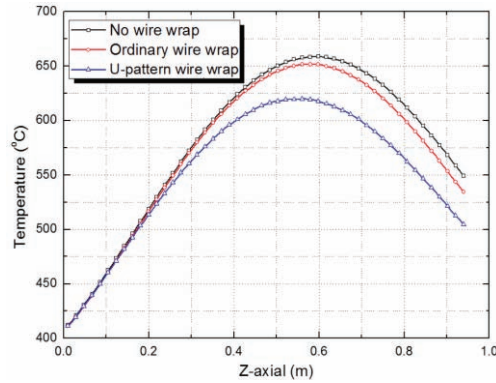


Figure 8. Axial temperature distribution of center fuel pin.

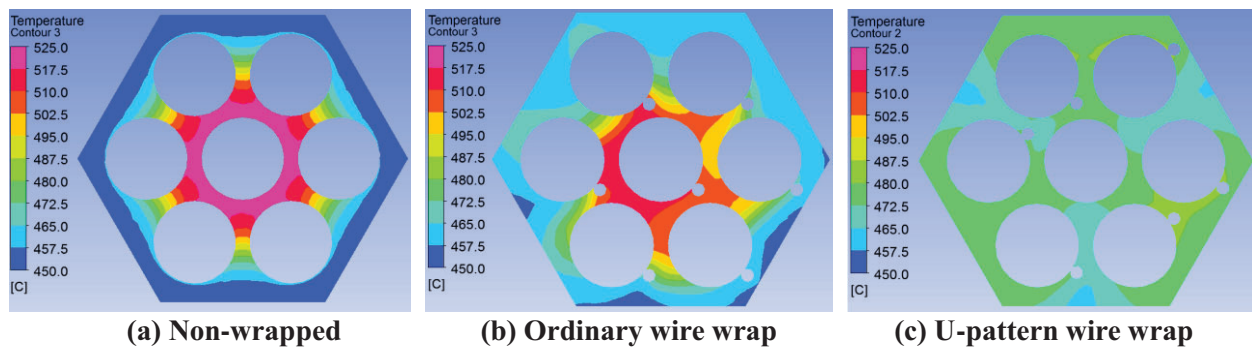


Fig. 9. Temperature distribution of cross section ($z = 0.8$ m) at different sub-channel conditions.

3.3. Velocity distribution in the bundle

Figure 10 shows the sodium velocity distribution and the velocity vector at a height of 0.8m. The transverse velocity is shown, rather than the velocity in the inlet direction, as the transverse velocity is related to coolant mixing. The maximum transverse velocity of the ordinary wire-wrapped pin case is higher than that of the U-pattern case. The average transverse velocities for the non-wrapped, ordinary, and the U-pattern cases are 0, 0.038, and 0.019 m/s, respectively. The rotational motion of the sodium coolant is generated by the wire-wrapped pin geometry. In the ordinary wire-wrap geometry, counter flow could potentially be generated in all sub-channels, as shown in figure 3. This prediction was confirmed by observing the velocity vector. Although the flow velocity is high, the flow pattern is complicated in the sub-channels around the center pin. A fast and stable flow pattern could be observed near the hexagonal walls. The direction of this rotating flow is dependent on the winding direction of wires. The sodium coolant that is adjacent to the hexagonal walls is relatively cold, and this coolant should flow into the sub-channels around the center pin. However, this flow is limited due to the reverse flow caused by the wire-wrapped spacers. Because of this flow pattern, the temperature reduction of the coolant with the ordinary wire wrap is insufficient compared with the non-wrapped fuel pin. The flow direction of the U-pattern is different. The expected flow pattern, which is presented in figure 4, was observed. The mixing of coolant would be maximized in this condition, and a uniform temperature distribution results. Although locally faster velocity regions are generated in figure 10(b), the U-pattern pins arrangement provides suitable coolant flow to remove the heat from the fuel pins, as shown in figure 10(c). A stable coolant flow was observed in all sub-channels.

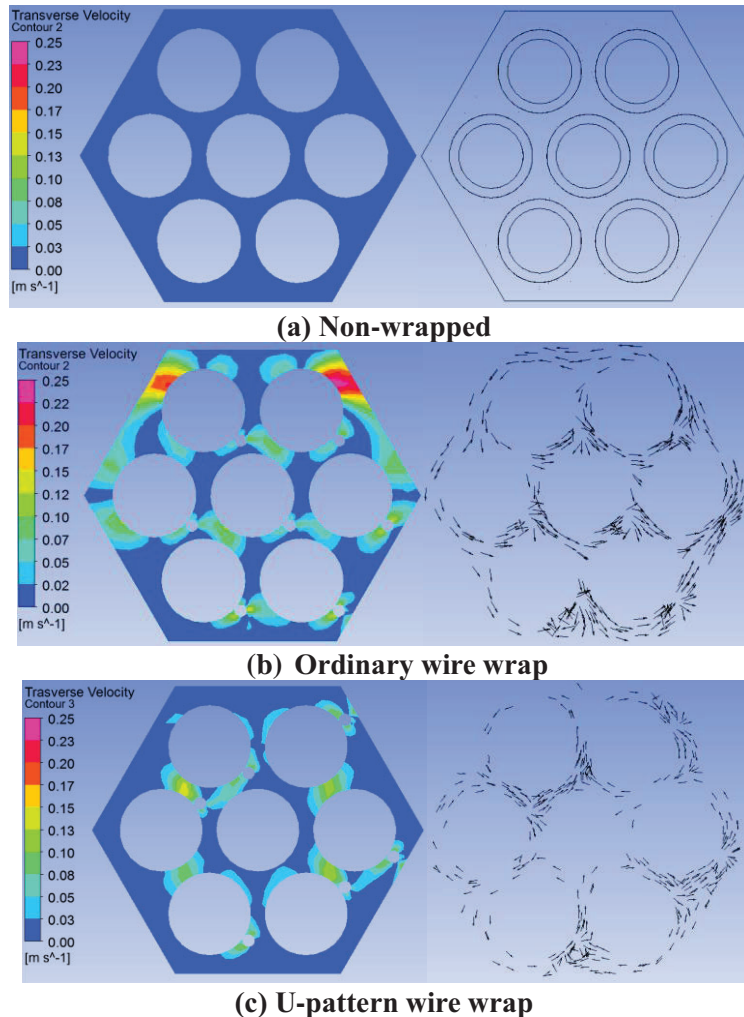


Figure 10. Transverse velocity distribution and velocity vector of cross section ($z = 0.8$ m) at different sub-channel conditions.

3.4. Heat transfer coefficient and Nusselt Number

Table II shows the calculated heat transfer coefficient from the CFD analysis. The heat transfer coefficient was increased due to the wire wrap. The geometry of the wire wrap causes turbulent flow in the sub-channels. The value of the heat transfer coefficient for both the ordinary wire wrap and the U-pattern is similar. Although the average transverse velocity for the ordinary wire-wrap geometry is higher, the heat transfer would deteriorate due to locally complicated flow patterns.

Equation (1) expresses the heat flow in the fuel. Equation (1) is one-dimensional heat conduction equation. This equation was generally used to calculate the pin center temperature. It is assumed that the volumetric heat source is constant and the interfacial gap and contact resistance is neglected in Eq. (1). Assuming that the temperature of the sodium coolant is fixed, an increased heat transfer coefficient, would reduce the temperature difference. The maximum fuel temperature could therefore be reduced in the geometry which has the ordinary wire wrap. The case of the geometry with the U-pattern is different. If there is considerable mixing in the sub-channels, then the temperature of the coolant could be decreased. This phenomenon could be applied in the geometry with the U-pattern. Ultimately, the

maximum fuel temperature could be reduced by considering the enhanced heat transfer and relatively cold coolant.

$$T_m - T_f = \frac{q''' R^2}{4\pi k_f} + \frac{q''' R^2}{2} \left[\frac{1}{k_c} \ln \frac{R+c}{R} + \frac{1}{h(R+c)} \right] \quad (1)$$

The dominant heat transfer mode on the heater pin surface is convection. Equation (2) shows the general expression for convection heat transfer with respect to Nu. ΔT is defined as the difference in temperature between the surface of a central pin and a triangular sub-channel surrounding this pin. The information for the heat flux could be obtained from post-processing the CFD results. Although the boundary condition of a pin (like the temperature of sodium coolant) is different for each case, the heat flux profile is very similar. The value of Nu for each case is indicated in figure 11. It is confirmed that the stable cross flow was generated in the case 3. The intensity of this cross flow in the specific location was determined by the pattern of the adjacent wire spacers. The high Nu number means that the intensity of the cross flow is strong. As a result, well-mixed flow was formed without much temperature difference as shown in Fig. 12. The meaning of the high Nu number for the case 3 is suitable to become the well-mixed state. The result of the non-wrapped case is compared with Eq. (3). Kazimi and Carelli conducted sub-channel analysis with the coolants Na, Hg, and NaK to develop this correlation. Equation (3) is based on a theoretical analysis and best fit of available experimental data through rod bundles with pitch-to-diameter ratios between 1.15 and 1.30. The value of Nu for the non-wrapped case is in good agreement with Eq. (3). The Péclet number (Pe) is influenced by the temperature-dependent density, dynamic viscosity, thermal conductivity, and heat capacity of sodium in Eq. (3). The inlet and outlet temperature of the sodium is 390 °C and 540 °C, respectively. The maximum variation of Nu number is about 3% over this temperature range.

In the non-wrapped case, the change in Nu could be divided into three parts, which are the developing, steady, and developed region. In the developing region, the sodium coolant is sufficiently cold to accelerate the heat transfer between the heated wall and the sodium. The steady region is where a rapid increase of temperature occurs in the fuel pin and sodium coolant simultaneously. This is caused by the cosine shape of the normalized heat generation curve, where the heat generated at the middle of the pin is higher than the edge regions. In the developed region, the trend of heat transfer is the reverse of the developing region. The bulk temperature of sodium coolant increased continuously through passing the sub-channel with low power generation, and a negative heat transfer condition was formed in this region. This division could also be applied to the ordinary wire-wrap case. Transverse flow is naturally generated by the wire-wrapped spaces. The energetic mixing could be estimated by analyzing the periodic jumping of Nu. In the developing region, the value of Nu of the ordinary wire wrap is three times higher than that of non-wrapped case. The increase ratio continuously decreases according to the distance of sub-channel. Figure 12 shows the temperature distribution between the center of the fuel pin and the triangular sub-channel at $z = 0.436$ m and $z = 0.8$ m. The value of Nu with the ordinary wire wrap is lower than that with the non-wrapped wire at $z = 0.8$ m, as shown in figure 11. The temperature gradient of the ordinary wire wrap is relatively steep in comparison with that of the non-wrapped case. Although the calculated Nu of the ordinary wire wrap is low, the pin surface temperature is still relatively cold. These regions could be formed because of improper transverse flow. Counter flow occurred in the ordinary wire-wrap pattern. The hottest sodium was located in the central region of the fuel bundle. If flow direction in the sub-channels surrounding the center pin is toward the center of the fuel bundle, then a noticeable temperature difference could be observed, as shown in figure 12(a). Active convective heat transfer was generated at $z = 0.436$ m. The temperature gradient in the non-wrapped case is significantly higher than found in the ordinary wire-wrap case [9]. These two patterns of heat transfer for the ordinary wire-wrap case are

periodically repeated. A partially negative heat transfer could be compensated by transfer from the other active heat transfer regions.

The U-pattern demonstrates unique heat transfer. The trend of change for Nu is similar to the case of the ordinary wire wrap. The minimum value of Nu is always higher than that of the non-wrapped case. An unrealistic value of Nu was calculated due to highly active heat transfer. This is caused by the superb coolant mixing. There is no continuous decrease of Nu, regardless of flow length. A relatively low value of Nu in initial region was observed due to the undeveloped transverse flow. However, this geometry condition is different from a real fuel pin geometry; there is a part of the lower end plug and shielding in a real fuel pin. This region is also wrapped with wire spacer. Before entering the sub-channel of the fuel slug, which is the active fuel region, transverse flow could develop.

Table II. Heat transfer coefficient and pressure drop in CFD results.

	Heat transfer coefficient (W/m ² K)	Pressure drop (Pa)
Non-wrapped	3.565	22864
Ordinary wire wrap	3.878	34790
U-pattern	3.893	31321

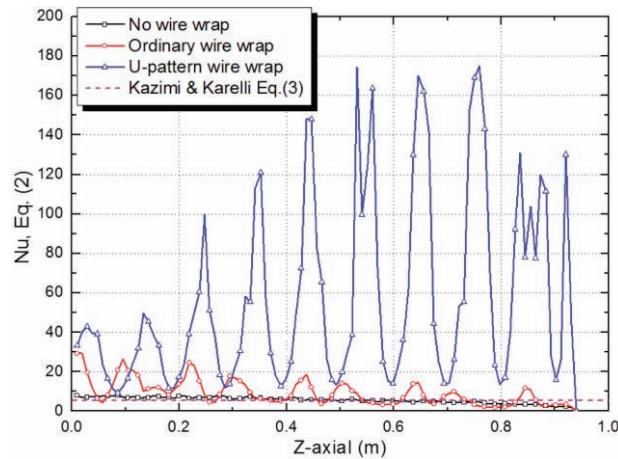
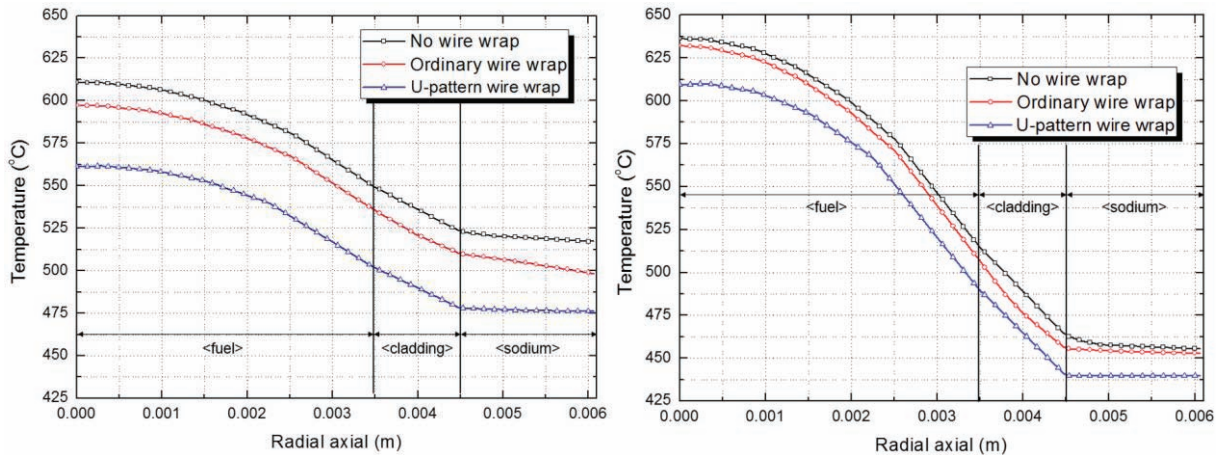


Figure 11. Nu variation along axial direction of fuel pin.



(a) $z = 0.436 \text{ m}$

(b) $z = 0.8 \text{ m}$

Figure 12. Temperature distribution of fuel and coolant according to lateral direction.

$$Nu = \left(\frac{q''}{\Delta T} \right) \left(\frac{d_h}{k} \right) \quad (2)$$

$$Nu = 4 + 0.33 \left(\frac{P}{D} \right)^{3.8} \left(\frac{Pe}{100} \right)^{0.86} + 0.16 \left(\frac{P}{D} \right)^{5.0} \quad (3)$$

$$\text{for } 1.15 \leq \frac{P}{D} \leq 1.3 \text{ and } 10 \leq Pe \leq 5000$$

3.5. Pressure drop and friction factor

Figure 13 shows the change of the static pressure in a sub-channel for each case. A fluctuating static pressure was observed in the case of the ordinary wire wrap arrangement. This is caused by the complicated flow in the sub-channels. There is a relative smooth line in the U-pattern case, because of the favorable flow pattern for coolant mixing. One of the disadvantages of wire wrapping is the increased pressure drop. Approximately 52% additional pressure drop was calculated in CFD simulation due to the ordinary wire wrap. A high-performance pump would be required to maintain the coolant flow at normal operation conditions. The U-pattern could reduce the pressure drop in comparison with one of the ordinary wire-wrap geometries. The friction factor for each CFD case can be calculated with Eq. (4). Table III shows a comparison of the results of the CFD analysis performed on some models with a 7-pin wire-wrapped fuel bundle. Some friction models and each calculated values are summarized in Table III. There are based on the theoretical or experimental analysis with different assumption and measuring position. Although the friction factor was calculated with same geometry and condition, the values are varied with a wide range. However, the value of friction factor obtained from the CFD analysis of this work is in the range of values shown in Table III. The friction fraction of the non-wrapped case (Case 1) was compared with the result calculated by the Colebrook equation, and a difference of approximately 13% was found. The surface is assumed as smooth condition ($\epsilon/De=0$). The friction factor for the Rehme model has relatively lower value than that used in the Colebrook equation. The sub-channel geometries were divided to three types (interior, edge, and corner) in the Novendstem and C-T (Cheng and Todreas) models. The friction factor of the interior was used as the overall friction factor to determine the pressure drop in the fuel bundle in the Novendstem model. However, the C-T model presents two types of calculation method. The simplified C-T model is similar to the Novendstem model, and the overall friction factor was determined by the simplified method. The alternative is to calculate the friction factor separately for each geometry type. The position of the wire wrap is an important parameter. The friction factor of the C-T model was calculated in the condition that the wire wrap is located at 0° . Case 2 is the friction factor of the ordinary wire wrap from CFD analysis. This value is similar to the value obtained from the Engel, Markley, and Blashop model. The U-pattern geometry reduces the pressure drop by approximately 10%. The pressure drop in the U-pattern is lower because there is no wire-wrapped spacer

at the center pin, and a stable flow pattern is formed. We present the modified Engel, Markley, and Blaschop model, Eq. (5), to predict the friction factor of the U-pattern.

Table III. Comparison with friction factor model for wire-wrapped pin bundle

	Friction factor		Friction factor
Case1 (non-wrapped)	0.0229	Engel, Markley and Blaschop model [12]	0.0347
Case2 (ordinary)	0.0348	Cheng and Todreas model [2], interior ($\theta = 0$)	0.0242
Case3 (U-pattern)	0.0314	Cheng and Todreas model, edge ($\theta = 0$)	0.0203
Colebrook equation [10]	0.0199	Cheng and Todreas model, corner ($\theta = 0$)	0.0206
Novendstern model [1]	0.0251	Cheng and Todreas model, simplified	0.0268
Rehme model [11]	0.0191	Sobolev model [13]	0.0247

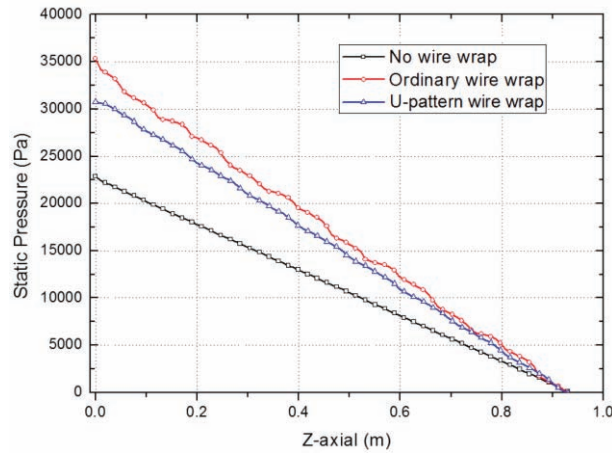


Figure 13. Static pressure at center of triangular sub-channel.

$$\Delta P = f \left(\frac{L}{D_e} \right) \frac{\rho V^2}{2} \quad (4)$$

for $Re > 4000$

$$f = \frac{0.495}{Re^{0.25}} \quad (5)$$

4. CONCLUSIONS

A modified wire-wrap geometry was presented to increase the heat transfer from heated fuel pins. A combination of a non-wrapped pin and pins with alternating winding direction allows a uniform temperature distribution to form. The reduction of maximum temperature was observed in CFD results, caused by the enhanced mixing of coolant. The presented unique pattern lowers the pressure drop compared with that of the ordinary wire wrap geometry. The new wire-wrapping arrangement could enhance the efficiency of LMFBR, by simultaneously satisfying the conditions of low pressure drop and high heat transfer.

NOMENCLATURE

C	thickness of cladding
d_h	hydraulic diameter
D	diameter of pins
h	heat transfer coefficient on the wall
k	thermal conductivity of sodium coolant
k_c	thermal conductivity of cladding
k_f	thermal conductivity of fuel
Nu	Nusselt number
T_f	coolant temperature
T_m	maximum fuel temperature
P	pitch of fuel pins
Pe	Péclet number.
q'''	volumetric thermal source
R	radius of fuel

ACKNOWLEDGMENTS

This work was supported by the Nuclear Energy Research Program through the National Research Foundation of Korea (NRF) funded by the Ministry of Science, ICT, and Future Planning (2013M2B2B1075734, 2013M2A8A1041442)

REFERENCES

1. E. Novendstern, "Turbulent flow pressure drop model for fuel rod assemblies utilizing a helical wire-wrap spacer system," *Nuclear Engineering and Design*, **22**, pp. 28-42 (1972)
2. S.K. Cheng, N.E. Todreas, "Hydrodynamic models and correlations for bare and wire-wrapped hexagonal rod bundles - bundle friction factors, subchannel friction factors and mixing parameters," *Nuclear Engineering and Design*, **92**, pp. 227-251 (1986)
3. R. Gajapathy, K. Velusamy, P. Selvaraj, P. Chellapandi, S. Chetal, "A comparative CFD investigation of helical wire-wrapped 7, 19 and 37 fuel pin bundles and its extendibility to 217 pin bundle," *Nuclear Engineering and Design*, **239**, pp. 2279-2292 (2009)
4. K.D. Hamman, R.A. Berry, "A CFD simulation process for fast reactor fuel assemblies," *Nuclear Engineering and Design*, **240**, pp. 2304-2312 (2010)
5. V.Y. Volkov, O. Belova, A. Krutikov, A. Skibin, "coolant flow simulation in fast reactor wire-wrapped assembly," *Thermal Engineering*, **60**, pp. 429-433 (2013)
6. M. Talebi, R. Abdolahi, A.A. Nadooshan, "Investigation of effects of helical wire-wrapped spacers on thermo hydraulic properties of a fluid flow along to heated fuel bundle," in: *Proceedings International Journal of Application or Innovation in Engineering & Management (IJAIEEM)*, pp. 388-398 (2014)

7. D.H. Hahn, Y.I. Kim, Y.G. Kim, "KALIMER-600 conceptual design report," in: *KAERI/TR-3381*, Korea Atomic Energy Research Institute, Daejeon (Korea, Republic of) (2007)
8. Y. Kim, J. Jang, J. Lee, S. Kim, S. Kim, J. Kim, H. Jung, H. Lee, "Conceptual design report of SFR Demonstration Reactor of 600MWe capacity," in, *KAERI/TR-4598*, Korea Atomic Energy Research Institute, Daejeon (Korea, Republic of) (2012)
9. M. Kazimi, M. Carelli, "Heat transfer correlations for analysis of CRBRP assemblies," *Atomic Energy Review*, **18**, pp. 329-552 (1980)
10. C.F. Colebrook, "Turbulent Flow in Pipes, with particular reference to the Transition Region between the Smooth and Rough Pipe Laws," *Journal of the ICE*, **11**, pp. 133-156 (1939)
11. K. Rehme, "Pressure drop correlations for fuel element spacers," *Nuclear technology*, **17**, pp. 15-23 (1973)
12. F. Engel, R. Markley, A. Bishop, "Laminar, transition, and turbulent parallel flow pressure drop across wire-wrap-spaced rod bundles," *Nuclear Science and Engineering*, **69**, 290-296 (1979)
13. V. Sobolev, "Fuel rod and assembly proposal for XT-ADS pre-design," in: *Coordination meeting of WP1&WP2 of DMI IP EUROTRANS*, Bologna, pp. 8-9 (2006)